Bulletin of the Seismological Society of America, Vol. 98, No. 4, pp. 1964–1974, August 2008, doi: 10.1785/0120070131

Recalibration of the Magnitude Scales at Campi Flegrei, Italy, on the Basis of Measured Path and Site and Transfer Functions

by Simona Petrosino, Luca De Siena, and Edoardo Del Pezzo

Abstract New duration-based local (M_L) and moment (M_w) magnitude scales are obtained for the Campi Flegrei area through analysis of a dataset of local volcano-tectonic earthquakes. First, the *S*-wave quality factor for the investigated area was experimentally calculated, and then the distance-correction curve, $\log A_0(r)$, to be used in the Richter formula $M_L = \log A_{max} - \log A_0(r)$, was numerically estimated by measuring the attenuation properties and, hence, propagating a synthetic *S*-wave packet in the earth medium. The local magnitude scale was normalized to fit the Richter formula that was valid for Southern California at a distance of 10 km. M_L was estimated by synthesizing Wood–Anderson seismograms and measuring the maximum amplitude. For the same dataset, the moment magnitude was obtained from *S*-wave distance-corrected and site-corrected displacement spectra. Comparisons between local and moment magnitudes determined, along with the old duration magnitude (M_D) routinely used at the Istituto Nazionale di Geofisica e Vulcanologia–Osservatorio Vesuviano, are presented and discussed. Moreover, the relationships between M_L and M_w calculated for two reference sites are also derived.

Introduction

The quantification of the seismic energy of earthquakes occurring in volcanic regions is of great importance to better our understanding of the dynamics of volcanoes. The amount of released energy and its variation during seismic crises can be assumed to be an indicator of the source processes that act inside the volcano. In this context, the effects of propagation in attenuative media should be considered, to correct for path effects and to correctly estimate the seismic energy released at the source. Moreover, the use of magnitude scales as homogeneous as possible for the seismic energy quantification is recommended, to allow a comparison with dynamic processes occurring at other volcanoes.

The problem of quantifying seismic energy is particularly crucial in densely populated areas, where the earthquake magnitude is one of the parameters used for the definition of the alert levels. Therefore, a correct magnitude estimate in high-risk volcanic areas has an important role for the monitoring activity. For all these reasons, in several studies in recent years there have been efforts to calibrate reliable magnitude scales for volcanic areas such as Mount Vesuvius, Deception Island, and Mount Etna (Del Pezzo and Petrosino, 2001; Havskov *et al.*, 2003; D'Amico and Maiolino, 2005).

Local and moment magnitude scales are the most widespread scales for the estimates of the earthquake energy, and they are commonly used by volcanological observatories and seismological agencies. Bulletins of current seismic activity often contain magnitude estimates based on these scales. The local scale proposed by Richter (1935) was the first to be introduced for earthquake size quantification. Initially developed for Southern California, this scale was soon extended to many other regions in the world (see, among others, Alsaker *et al.*, 1991; Kim, 1998; Gasperini, 2002; Baumbach *et al.*, 2003; Stange, 2006) after having found the correct distance-correction curves that empirically account for local attenuation. Worldwide, many seismic catalogs based on the local magnitude are available; therefore, this scale is useful for comparisons of seismic activity occurring in different regions.

On the other hand, Hanks and Kanamori (1979) proposed a new magnitude scale that was based on the estimate of the scalar seismic moment. This scale does not saturate for large earthquakes, it is independent of the distance-correction law, and it has to be considered the most reliable scale for earthquake size quantification. For this reason, many studies have developed relationships to express the local magnitude in terms of the moment magnitude (Bakun, 1984; Papazachos *et al.*, 1997; Grünthal and Wahlström, 2003; Bindi *et al.*, 2005; Scordilis, 2006).

At present, the seismological practice of the Istituto Nazionale di Geofisica e Vulcanologia–Osservatorio Vesuviano (INGV–OV) calculates the magnitude of earthquakes occurring in the Campi Flegrei area from the coda duration measured at a short-period seismic station (STH; Fig. 1) located

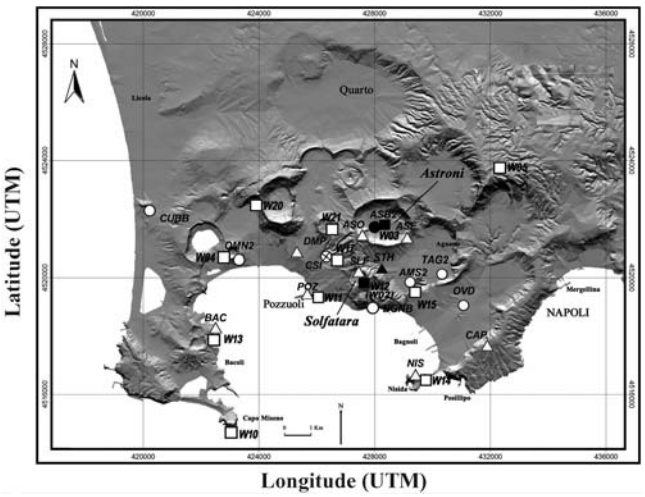

Figure 1. Map of Campi Flegrei with station positions. The different symbols correspond to digital broadband stations, circles; a digital short-period station, crossed circle; analog short-period stations, triangles; and digital short-period stations deployed by the University of Wisconsin in 1984, squares. Filled symbols correspond to the stations used in the present study for the determination of the new magnitude scales.

in the area of the Solfatara crater. It is well known that for local earthquakes, the duration of the seismograms is independent of the seismic source, the station-to-source distance, and the regional geology; it depends only on the energy of the seismic event (Sato and Fehler, 1998). The duration magnitude formula routinely used at the INGV–OV (Orsi *et al.*, 1999) is expressed as

$$M_D = -2.46 + 2.82 \log \tau, \tag{1}$$

where τ is the earthquake duration, measured from the *P*-wave arrival to the point at which the coda of the signal drops down the noise amplitude. The relation of equation (1) is purely empirical, and it can be used only for comparisons between local events.

In the present study, we introduce local and moment magnitude scales for the area of Campi Flegrei, to allow comparisons of the present day levels of seismicity with those measured for other active volcanoes.

Sometimes the original local magnitude scale developed by Richter (1935) for Southern California is used for different regions, when similar crustal attenuation properties are observed. This is not expected in the case of volcanic areas such as Campi Flegrei, where the quality factor (Q) values are lower than those of the surrounding tectonic areas. Therefore, to calibrate a reliable magnitude scale that fully takes into account the very local attenuation, we first perform a preliminary attenuation study for the investigated area, calculating the *S*-wave quality factor. Then, following Boore (1983), we generate synthetic wave packets with a source spectrum characteristic of the volcano-tectonic (VT) earthquakes that occur at Campi Flegrei and propagate in a medium with the attenuation parameters obtained. From the decay pattern of the maximum amplitude, we estimate the correct distance-correction curve and calibrate the local magnitude scale. Local magnitude is then computed by applying the new scale to real seismograms convolved with the response function of a Wood–Anderson seismometer.

Although the calibration of the local magnitude scale can be problematic at close distances, due to large uncertainties in the determination of the surface attenuation properties, a practical reason led us to introduce this scale for Campi Flegrei: amplitude-based magnitude measurements can be useful in this volcanic area, instead of the duration-based ones, when earthquake swarms occur and the estimation of the duration becomes difficult due to the occurrence of new events in the coda of the previous ones.

We also obtain more robust estimates of the earthquake energy by calculating the moment magnitude from the spectral amplitudes of the VT earthquakes, and we derive some of the relationships between the different duration-based and amplitude-based scales.

We carry out these tasks for two different reference sites, Solfatara and Astroni, to have alternative ways of estimating the magnitude and to overcome some practical problems, such as amplitude clipping, coda truncation for earthquakes occurring closely spaced in time, and malfunction of the reference station.

Instruments, Seismicity, and Dataset

The present seismic monitoring network of the Campi Flegrei volcanic complex managed by the INGV–OV is composed of nine analog stations that are telemetered to the Data Acquisition Center and eight digital stations (four Lennartz MarsLite, three Lennartz M24, and one Lennartz PCM 5800) recording *in situ*. The analog stations are equipped with vertical short-period 1-Hz Mark L4-C sensors or three-component 1-Hz Mark L4-3D or Geotech S13 sensors. Signals are sampled at 100 Hz. The digital network is equipped with three-component broadband Lennartz LE3D/20s or Guralp CMG40T/60s seismometers, except for the one Lennartz PCM 5800 station, which is equipped with a three-component 1-Hz Geotech S13 geophone. The sampling rate of the digital stations is set to 125 Hz.

The seismicity of Campi Flegrei, which generally occurs during the phases of uplift, has mostly been characterized over the last 25 yr by moderate-to-low duration magnitude (up to M_D 4.2) VT earthquakes, with epicentral locations in the area of the Solfatara crater and at depths of less than 5 km (Aster and Meyer, 1988).

The most important recent bradyseismic crisis at Campi Flegrei occurred in 1982–1984, when there was an uplift of 1.8 m that was centered on the town of Pozzuoli and that was accompanied by more than 16,000 earthquakes. Minor uplift episodes that were accompanied by seismic activity occurred in 1989, 1994, and 2000 (Orsi *et al.*, 1999; Saccorotti, 2007). The most recent phase of unrest started in November 2004,

and it was characterized by the occurrence of VT and long-period seismicity (Saccorotti *et al.*, 2007). Approximately 300 low-magnitude VT earthquakes were recorded between March 2005 and December 2006, most of which were concentrated within distinct seismic sequences. The main seismic swarms occurred on 5 October 2005 (about 90 microearthquakes with M_{max} of 1.1) and during the period of 19–30 October 2006 (160 microearthquakes with M_{max} of 0.8).

To correctly calibrate the magnitude scales for the Campi Flegrei, we used the recordings from both the analog three-component STH station and the digital three-component ASB2 station (Fig. 1). The first of these is located in the Solfatara area and is equipped with a short-period 1-Hz Mark L4-3D sensor, while the other is located in the Astroni crater and is equipped with a broadband Lennartz LE3D/20s seismometer. The advantage of using the data recorded by a digital station with a high-dynamic range, such as for ASB2, is that amplitude saturation for large earthquakes is avoided. However, because STH is the reference station routinely used at the INGV–OV for duration magnitude determination, new magnitude relations should also be derived for this station to provide comparison with previous data and to ensure consistency and continuity within the seismic catalog.

The starting dataset consisted of 83 three-component recordings of local earthquakes that occurred in the period from March 2005 to December 2006. The events were located by applying a grid search algorithm and using a three-dimensional velocity model (Saccorotti *et al.*, 2007). This dataset was characterized by earthquakes with low M_D (up to 1.2); for this reason it was enlarged by the addition of a subset of earthquakes from the 1984 bradyseismic crisis that were chosen on the basis of location (occurring in approximately the same area as the 2005–2006 events) and magnitude (between 0.9 and 3.2). Using this whole dataset, the validity of the magnitude relations is ensured over a wider magnitude range.

The dataset collected during the 1984 bradyseismic crisis has been widely described in many studies (see, for example, Aster and Meyer, 1988; Aster *et al.*, 1992), as well as the recording network that was installed at that time by the University of Wisconsin. For the present analysis, we selected 57 earthquakes that were recorded at the W12 and W03 digital stations, which were equipped with three-component 1-Hz Hall-Sears geophones and a sampling rate of 100 Hz. These two stations were chosen due to their proximity to the STH and ASB2 stations, respectively (less than 1 km; Fig. 1). In this way, we can consider the datasets recorded at STH and W12 representative of the Solfatara site and those from ASB2 and W03 representative of the Astroni site.

The final full dataset used in the present study therefore consists of 140 earthquakes that were recorded in 1984 and 2005–2006 and that have hypocentral distances ranging from 0.2 to 8 km and depths ranging from 0 to 5 km.

This dataset was used to calibrate the duration magnitude relationships with the local and moment magnitudes at the reference site of Solfatara, using recordings from stations STH and W12. Moreover, we calculate the local and moment magnitudes for the earthquakes recorded at the digital stations ASB2 and W03 and introduce the relationships between M_L and M_w calculated for the Astroni and Solfatara areas, to provide an alternative reference site for the magnitude estimates without losing the consistency of the seismic catalog.

Methodology

Seismic Attenuation and Local Magnitude Determination

The original definition of local magnitude introduced by Richter (1935) is based on the equation

$$M_L = \log A - \log A_0(r), \tag{2}$$

where A is the maximum amplitude of the Wood–Anderson trace in millimeters and $\log A_0(r)$ is the distance-correction curve, which is defined with respect to a reference earthquake and needs to be experimentally determined. Because of the restricted number of stations recording the same event and the short distance range of our observations (0.2–8 km), it is difficult to experimentally derive the maximum amplitude decay with distance in the Campi Flegrei area. To overcome this difficulty, we used the method described by Del Pezzo and Petrosino (2001), which is based on the procedure of the simulation of a synthetic wave packet (Boore, 1983) for a suitable source-distance range in a medium with known attenuation properties.

As a preliminary step, we estimated the average value of the shear-wave quality factor for Campi Flegrei using part of the dataset (January–April) that was recorded during the 1984 bradyseismic crises at the seismic network installed in that period by the University of Wisconsin and the Osservatorio Vesuviano (see Aster *et al.*, 1992, for more details). The Q-value in the crust was determined by using the recordings of 195 local earthquakes that were recorded at the stations W12, W03, and W21 and that had focal depths from 0 to 5 km and hypocentral distances from 0.2 to 9 km.

The amplitude spectrum for the S and P waves as the product of source, path, and site effects can be written as

$$A_{ij}(f,r) = S_i^A(f)T_j(f)\exp(-\pi f k_0)G_{ij}(r) \times \exp\left(-\pi f \frac{t_{ij}(r)}{Q(f)}\right) I_j(f), \tag{3}$$

where $A_{ij}(f,r)$ is the high-frequency amplitude spectrum; f is the frequency of the P- or S-wave radiation emitted by the source i at a total distance r_{ij} measured along the source (i) station (j) ray path; $S_i^A(f)$ is the amplitude spectrum at the source; $T_j(f)$ is the site amplification function; $\exp(-\pi f k_0)$ is the site-dependent attenuation term or

diminution operator (the parameter k_0 determines the high-frequency spectral decay and depends on the local geology, as shown by Anderson and Hough [1984]); G_{ij} is the geometrical spreading term, which is assumed to be equal to r_{ij}^{-1}; $\exp[-\pi f t_{ij}(r)/Q(f)]$ is the path-dependent anelastic attenuation term and $Q(f)$ is the total quality factor averaged in the earth volume under investigation; t_{ij} is the travel time along the ray with coordinate r; and $I_j(f)$ is the instrument transfer function.

Following Abercrombie (1995), the earthquake source spectrum can be written as

$$S_i^A(f) = \frac{\Omega_0}{[1 + (f/f_c)^{\gamma n}]^{1/\gamma}},$$

where Ω_0 is the long-period amplitude, f is the frequency, f_c is the corner frequency, n is the high-frequency (log-log) fall-off rate, and γ is a constant. There will always be some ambiguity concerning the source spectral fall-off and attenuation. We can assume $n = 2$ for close events like those used in this study and a Boatwright spectral shape ($\gamma = 2$), which provides a better fit of our data:

$$S_i^A(f) = \frac{\Omega_0}{[1 + (f/f_c)^4]^{1/2}}.$$

The quality factor Q can be estimated by taking the logarithm and numerically differentiating equation (3), with the assumption that Q is constant over narrow frequency bands. Introducing the slowness $s_0 = 1/v_s$, we obtain

$$\begin{aligned} H_{ij} &= D_f(\ln A_{ij}) \\ &= -\frac{2f^3}{f_c^4 + f^4} + D_f[\ln T(f)] - \pi k_0 - \pi r_{ij} s_0 \frac{1}{Q^{ij}(r)} \\ &\quad + D_f[\ln I_j(f)], \end{aligned} \tag{4}$$

where the geometrical spreading term has disappeared, as it is independent of frequency.

We made a preliminary selection on the waveforms of our dataset, on the basis of the signal-to-noise ratio and the absence of spikes and other disturbances. Then, numerical differentiation was carried out for the average *S*-log-spectra obtained by using the two horizontal components of the seismograms. Before differentiating, we applied a smoothing to each spectrum using a moving window of seven points, with the sliding of one point. Finally, we selected only those spectra that showed a very clear decay pattern, and we visually measured the corner frequency. For each of the three stations, the site amplification function $T(f)$ with respect to the average site amplification (Fig. 2) and the k_0 term (Table 1) used in equation (4) had already been measured by Del Pezzo *et al.* (1993) and De Natale *et al.* (1987), respectively. In particular, the k_0 term used for station W12 is that reported by De Natale *et al.* (1987) for station W02, as these two seismometers were installed at the same site. The value of s_0 was obtained from the inverse of the *S*-wave velocity, v_s (1500 m/sec), as measured by Vanorio *et al.* (2005).

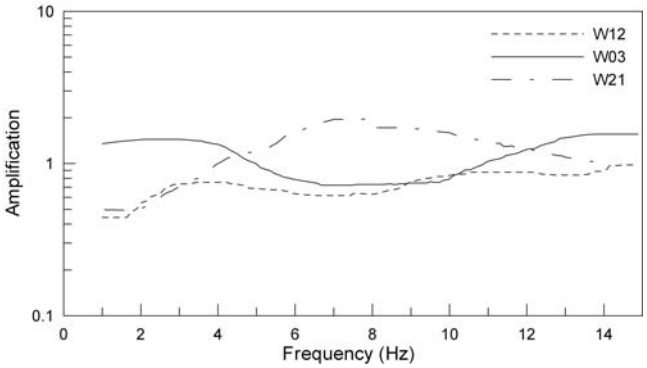

Figure 2. Site amplification functions for stations W12, W03, and W21 (after Del Pezzo *et al.*, 1993).

The system of equations (4) can be arranged in a matrix form (Menke, 1984):

$$\mathbf{d} = \mathbf{G}\mathbf{m}, \tag{5}$$

where $\mathbf{d}$ is the vector containing the data, $\mathbf{G}$ is the coefficient matrix, and $\mathbf{m}$ is the vector of the model parameters containing the unknown Q-values in the different frequency bands. We solved the inverse problem in 13 frequency bands with central frequencies C_f ranging from 3 to 15 Hz, with a step of 1 Hz and a bandwidth equal to $2(C_f/4)$.

To quantify the uncertainties that affect the estimation of the attenuation factor, we calculated the covariance matrix. In terms of the quantities defined in equation (5), the expression of the covariance matrix is

$$[\mathrm{cov}(\mathbf{m})] = \sigma_d^2[\mathbf{G}^{\mathrm{T}}\mathbf{G}]^{-1}, \tag{6}$$

where σ_d is the data variance that is calculated by propagating the uncertainties affecting each term of equation (4). Using the error estimates obtained by De Natale *et al.* (1987) and Del Pezzo *et al.* (1993) for the k_0 terms and the amplifications $T_j(f)$, and as the uncertainties that affect the spectral amplitudes and the corner frequencies are 20% and 25%, respectively, the percentage of standard deviation on the data vector $\mathbf{d}$ is 35%. By applying equation (6), the average relative error affecting the Q-values retrieved in each frequency band is 35%. The Q-values obtained show an

Table 1

k_0 Terms for Stations W12, W03, and W21 (after De Natale *et al.*, 1987)

Station	k_0
W12	0.004 ± 0.020
W03	0.022 ± 0.011
W21	-0.02 ± 0.023

overall frequency dependence (Fig. 3). To model the dependence of the quality factor on the frequency, we assumed the functional law $Q(f) = Q_0 f^g$. Then, the Q-values obtained were fitted to this relation, and we determined the parameters Q_0 and g and their errors. We found $Q_0 = 21 \pm 7$ and $g = 0.6 \pm 0.9$ (Fig. 3).

Once the frequency-dependent Q had been determined, we derived the maximum amplitude decay with distance for the definition of the distance-correction curve for the Campi Flegrei area. First, a synthetic wave train was generated by using the method of Boore (1983). A random number sequence with zero mean and a uniform distribution was multiplied in the time domain by a Hanning window, which accounted for the finite duration of the wave packet. Its amplitude spectrum was then multiplied by the source spectrum, with a spectral decay proportional to -2, a corner frequency of 13 Hz (the average corner frequency for earthquakes that constitute our dataset), and for the geometrical spreading, the anelastic attenuation and the diminution operators

$$\frac{1}{r}\exp\left(-\frac{\pi f r}{Q(f)v_s}\right)\exp(-\pi k_0 f).$$

In this way, we simulated an S-wave train generated by a Haskell-like source, propagating in a medium with a frequency-dependent Q and with k_0 equal to 0.008, which represents the average value of the k_0 parameters retrieved for the stations W03, W12, and W21 by De Natale *et al.* (1987). The synthetics were generated for a set of distances, r, in the 0.1–10 km range. Site amplification was introduced by multiplying the spectra by the term $T_j(f)$, where j represents the station index and is 1,2, because we calibrated the local magnitude scale for the two sites of Solfatara and Astroni. The site-corrected spectra were transformed into the time domain via inverse fast Fourier transform (FFT), and

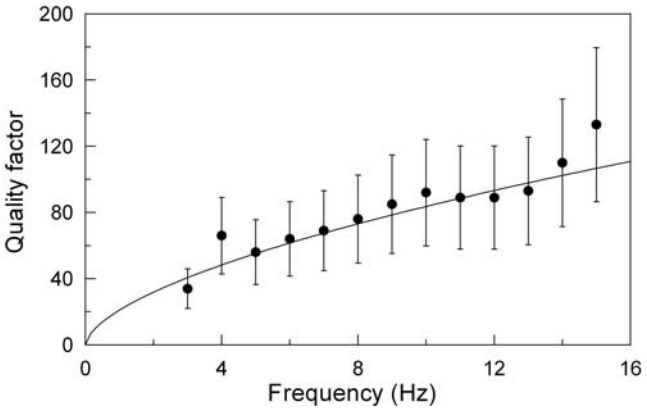

Figure 3. Quality factor (Q) values obtained from the attenuation analysis in the 3–15 Hz frequency range (circles), and the functional dependence on the frequency described by the law $Q(f) = 21f^{0.6}$ (solid line).

the maximum amplitudes corresponding to each distance r were fitted to the relationship

$$-\log A_{0j} = a\log r + br + c + \sum_{l=1}^{Ns} s_l \delta_{lj}, \qquad (7)$$

where δ_{lj} is the Kronecker delta and Ns is the number of stations (equal to 2). The system of equations (7) was inverted under the constraint that the station correction sum is equal to zero. In the inversion procedure, c was treated as a free parameter that will be determined by applying the normalization condition. The values obtained for the coefficients a and b and the station corrections, s_l, for the Solfatara and Astroni sites are

$$a = 0.95 \pm 0.08, \qquad b = 0.09 \pm 0.01,$$
$$s_{\text{solfatara}} = 0.12 \pm 0.03, \qquad s_{\text{astroni}} = -0.12 \pm 0.03.$$

The maximum amplitude decay with distance due to both geometric spreading and attenuation can therefore be expressed as

$$-\log A_0 = 0.95\log r + 0.09r + c. \qquad (8)$$

The value of the constant c was constrained to normalize the local magnitude scale to motions at small station-to-source distances. As demonstrated by Hutton and Boore (1987), the normalization distance of 100 km originally suggested by Richter might not be adequate when dealing with local earthquakes that are propagating in regions that have very different attenuation within the first 100 km. As we expect that for the Campi Flegrei volcanic complex the attenuation properties are quite different from those characterizing the surrounding area, we did not normalize at 100 km, but we choose the normalization distance of 10 km, which is the range in which we consider the attenuation properties modeled by both the $Q(f)$ and k_0 parameters to be reliable. Moreover, epicentral distances beyond 10 km are related to the tectonic seismicity of the Campanian Plain and of the Apennines, which is indeed excluded from our study.

Following Hutton and Boore (1987) for Southern California, the distance-correction curve for the reference earthquake of magnitude 3 is expressed as

$$-\log A_0 = 1.1\log(10/100) + 0.00189(10-100) + 3$$
$$\Rightarrow -\log A_0 = 1.72.$$

By substituting this value in (2), we can calculate the value of $\log A$ for the reference earthquake:

$$3 = \log A + 1.72 \Rightarrow \log A = 1.28.$$

On the other hand, if we take into account the distance-correction term derived for Campi Flegrei (see equation 8), and assuming that at the distance R_{ref} of 10 km an earthquake

of magnitude 3 would have the same amplitude as in Southern California on a Wood–Anderson seismometer, we can rewrite equation (2) as

$$3 = 1.28 + 0.95 \log R_{\text{ref}} + 0.09 R_{\text{ref}} + c,$$

and the value of the constant c becomes

$$c = -0.1 \pm 0.1.$$

Therefore, the local magnitude scale for Campi Flegrei is given by

$$M_{\text{L}} = \log A + 0.95 \log r + 0.09 r - 0.1 + s_j. \qquad (9)$$

To calculate the local magnitudes for the earthquakes of our dataset, we proceeded in the following way. For each of the 140 earthquakes, we calculated the Fourier transform of the two horizontal components and corrected them for the complex instrument transfer function. For the Mark-L4C, the response curve was obtained through a calibration procedure, while for the Lennartz LE3D/20s and Hall-Sears sensors we used the parameters reported in the data sheet. The corrected displacement spectra were then multiplied by the complex Wood–Anderson transfer function. We used the standard Wood–Anderson transfer function, with magnification of 2800, damping factor of 0.8, and natural period of 0.8 sec (Richter, 1935).

The synthetic Wood–Anderson seismograms (Fig. 4) were obtained by applying the inverse FFT algorithm, the zero-to-peak maximum amplitudes were measured on both of the horizontal components, and the two values were averaged. The local magnitude was estimated using equation (9). The error on the magnitude values was obtained by propagating the uncertainties that affect the maximum amplitude A, the hypocentral distance r, and the parameters a, b, c, and s_l of equation (7). Assuming that the distance estimates are affected by uncertainties on the order of 20% and that the relative error on the maximum amplitude is proportional to the signal-to-noise ratio (Del Pezzo and Petrosino, 2001), we found that the magnitude estimates are affected by an absolute error of 0.2, for a signal-to-noise ratio greater than 10. When the signal-to-noise ratio drops below 10, the absolute error on M_{L} increases to 0.3–0.4.

To show that our data fit to the attenuation model, we grouped the earthquakes of the dataset into three magnitude bins centered on M_{L} 1, 2, and 3, with a width on the order of the maximum absolute error on M_{L}, and then plotted the amplitudes of these earthquakes as a function of the distance (Fig. 5). The distribution of the observed amplitudes follows the theoretical attenuation law (equation 8) derived from ground-motion simulation. The distance-correction curve that is calibrated for the reference earthquake of magnitude 3, fits the observed amplitudes of the earthquakes well, with M_{L} in the 2.8–3.2 range.

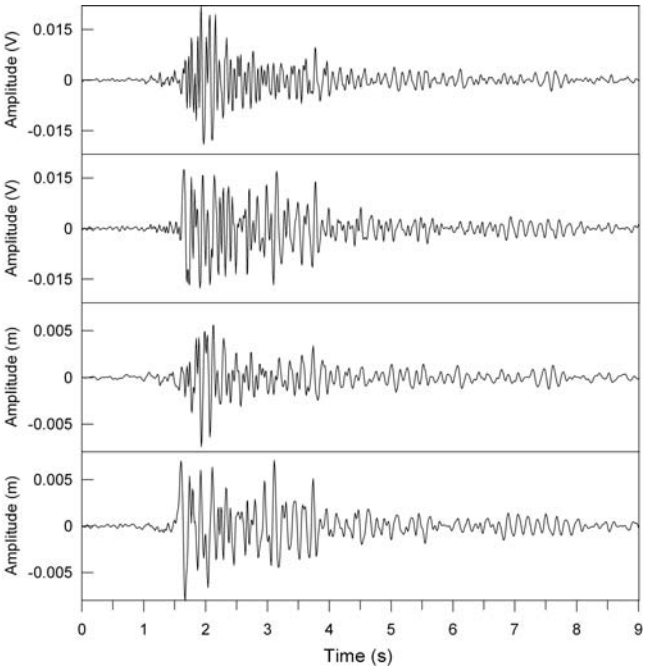

Figure 4. An example of a seismogram for a local VT earthquake. The upper panels represent the east–west and north–south components of the original velocity seismogram recorded at station ASB2. The lower two panels are the synthesized Wood–Anderson seismograms for the east–west and north–south components, respectively.

As we are interested in calibrating duration-based magnitude scales to allow rapid magnitude estimations for routine purposes, we also calculated the coda duration of all the earthquakes of the dataset recorded at the STH and W12 stations. As an objective criteria to adopt in measuring the earthquake duration, we calculated the root mean square (rms) value of the amplitude of the signal in a 0.5-sec-length sliding window, starting 2 sec before the P-wave arrival and multiplying this quantity by the time t. The function obtained

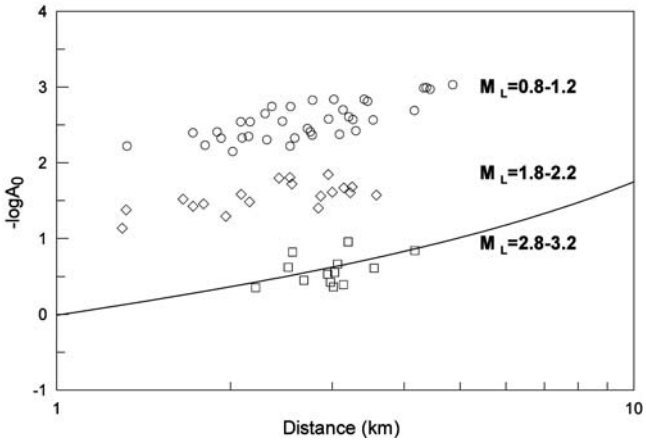

Figure 5. Observed amplitudes for three magnitude bins (M_{L} 0.8–1.2, circles; M_{L} 1.8–2.2, diamonds; and M_{L} 2.8–3.2, squares) and theoretical distance-correction curve (solid line).

rms × t, when plotted versus time, has a rapid increase that corresponds to the P-wave first arrival. Then, it decreases along the seismograms, and finally, it has a new increase when calculated after the coda end. By reading the time of the occurrence of the minimum, the earthquake duration can be obtained (Fig. 6). The corresponding duration magnitude can be estimated from equation (1).

Determination of the Moment Magnitude

We calculated the moment magnitude from the seismic moment M_0 using the formula of Hanks and Kanamori (1979):

$$M_w = \frac{\log M_0}{1.5} - 10.73. \quad (10)$$

With the hypothesis of a double couple mechanism, the scalar seismic moment M_0 can be estimated by the following relation (Lay and Wallace, 1995):

$$M_0 = \frac{4\pi\rho v_s^3 r\Omega_0}{FY_{\theta,\phi}}, \quad (11)$$

where r is the hypocentral distance, v_s is the average S-wave velocity in the medium between the source and the receiver, ρ is the average density, Ω_0 is the low-frequency level of the S-wave displacement spectrum, F is the free surface operator, and Y is the radiation pattern term.

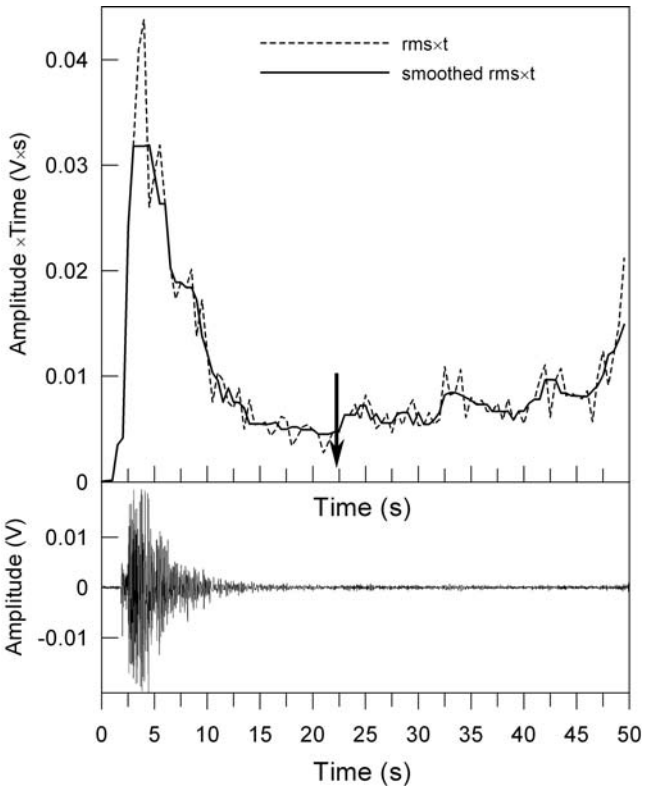

Figure 6. The function rms × t (dotted line) calculated for the seismograms shown in the lower panel is given. A smoothing over five points was applied (continuous line) before picking the earthquake cutoff time, marked by the arrow.

To estimate the seismic moment M_0 of the 140 earthquakes recorded at the STH, ASB2, W12, and W03 stations, we selected a 2.5-sec-long time window around the S-wave onset, and we calculated the amplitude spectrum of the displacement and corrected it for the geometrical spreading $1/r$, for the path-dependent anelastic attenuation term $\exp[-\pi rf/v_sQ(f)]$, for the diminution factor $\exp(-\pi k_0 f)$, and for the frequency-dependent site amplification $T(f)$. We used $k_0 = 0.004$ for stations W12 and STH and $k_0 = 0.022$ for stations W03 and ASB2 (Table 1), as W12 and STH are representative of the Solfatara site and W03 and ASB2 are representative of the Astroni site. For the same reason, the frequency-dependent site amplifications for STH and ASB2 were chosen to be equal to the amplification functions calculated with respect to an average site for stations W12 and W03, respectively (Fig. 2). We averaged the corrected spectra of the two horizontal components and evaluated the spectral level below the corner frequency. Finally, by applying equation (11) with the parameters listed in Table 2, we evaluated the scalar seismic moment associated with the double couple mechanism. To estimate the error on the moment magnitude, we propagated the uncertainties affecting the low-frequency spectral level, the $Q(f)$ value, the distance (20%), the velocity of S waves (20%), and the k_0 and $T(f)$ site terms reported in De Natale *et al.* (1987) and Del Pezzo *et al.* (1993), respectively. The variance $\sigma(\Omega)$ of the low-frequency spectral level was calculated following Boatwright (1978), from the noise spectrum $A(n)$, according to

$$\sigma(\Omega) \approx \frac{A(n)}{2}.$$

An absolute error of 0.2 was finally obtained for the moment magnitude estimates.

Regression and New Magnitude Scales

The comparison of the different magnitude scales is reported in Figure 7, where the local and moment magnitudes are reported as a function of the duration magnitude, for the reference site of Solfatara. The scatter of the points is caused by the uncertainty in the duration estimates, which is mainly related to the presence of noise and which mostly affects short-duration (less-energetic) earthquakes.

Table 2
Parameters Used for the Evaluation of the Seismic Moment

Parameter	v_s	ρ	F	Y
Value	1500 m/sec	2700 g/cm^3	2	0.63

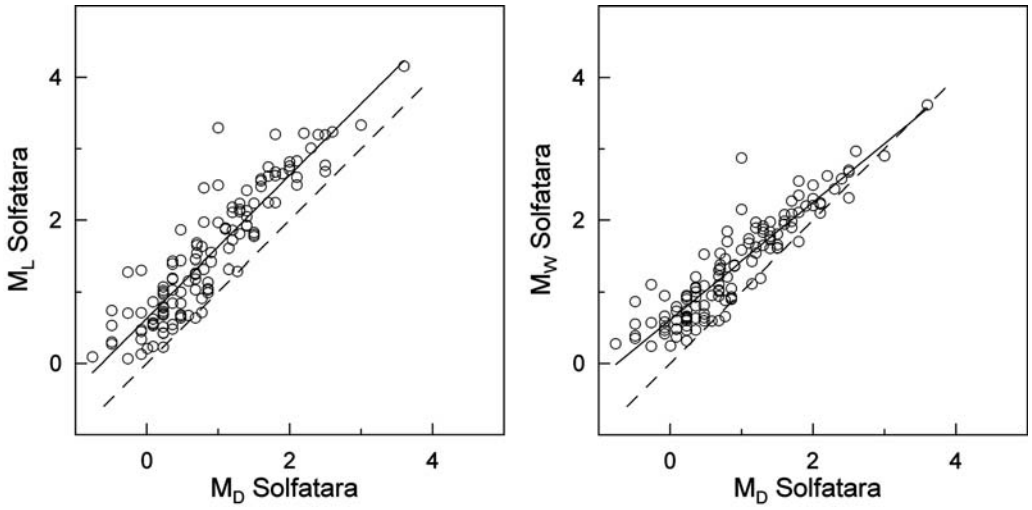

Figure 7. Left: The relationship between the local and duration magnitudes for the Solftara site. Right: The same for the moment magnitude. The dashed line represents the 1:1 relation.

The relationships between M_L, M_w, and M_D were derived from the linear fit:

$$M_L = 0.63(\pm 0.05) + 1.00(\pm 0.04)M_D,$$
$$M_w = 0.61(\pm 0.04) + 0.82(\pm 0.03)M_D.$$

The duration-based local and moment magnitude scales for the Solfatara site that can be used for practical purposes were obtained by linear regression on the logarithm of the coda duration:

$$M'_L = -1.8(\pm 0.1) + 2.8(\pm 0.1)\log\tau, \qquad (12)$$

$$M'_w = -1.4(\pm 0.1) + 2.3(\pm 0.1)\log\tau. \qquad (13)$$

The apex indicates that local and moment magnitudes (which are generally expected to be calculated from the amplitude and the seismic moment, respectively) are instead derived from the coda duration. In Figure 8, a comparison among the different duration-based scales is given for the Solfatara site. We can see that the duration magnitude, routinely calculated by using (1), and the moment magnitude differ for durations of up to 80 sec. In contrast, local magnitude systematically produces higher values with respect to the duration magnitude. This almost constant offset depends on the normalization criteria chosen to calibrate the local scale. The relationship between M_L and M_w was obtained by a linear regression (Fig. 9):

$$M_L = -0.12(\pm 0.02) + 1.23(\pm 0.01)M_w.$$

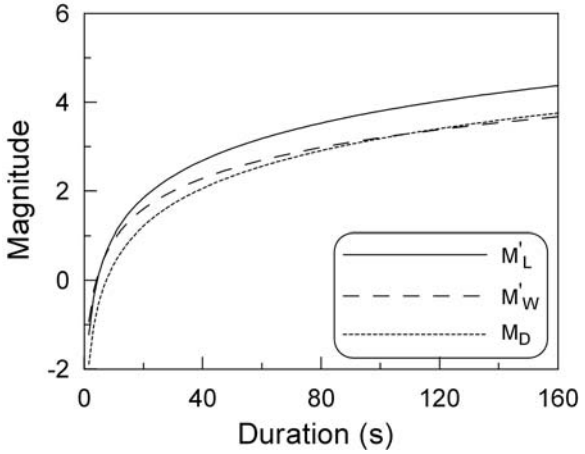

Figure 8. Local, moment, and duration magnitude laws, as a function of the coda duration.

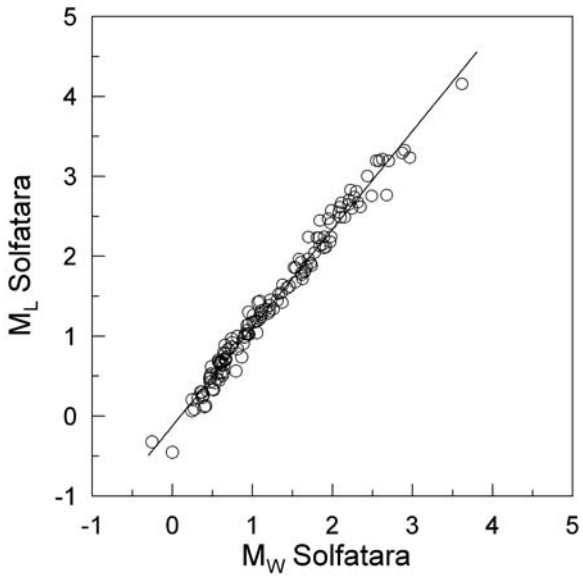

Figure 9. The relationship between the local and moment magnitudes derived for the Solfatara site.

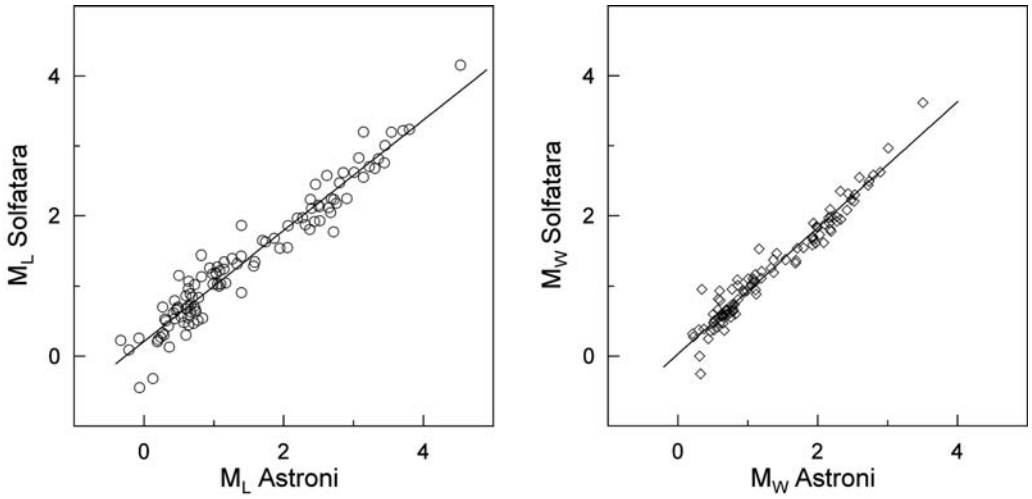

Figure 10. Left: The relationship between the local magnitudes for the Solfatara and Astroni sites. Right: The same for the moment magnitudes.

This result is similar to that found by Hanks and Boore (1984) for small earthquakes in California. Interestingly, to give alternative magnitude scales to be used in case of a malfunction of the STH reference station without loosing the catalog coherency, we derived the relationships for the local and moment magnitude between the Astroni and Solfatara sites. In this way, possible bias due to residual site effects can be taken into account. In Figure 10, M_L and M_w for the Astroni and Solfatara sites are shown. The relationships that relate the magnitudes calculated at the two sites are

$$M_L^S = 0.21(\pm 0.04) + 0.79(\pm 0.02) M_L^A, \qquad (14)$$

$$M_w^S = 0.028(\pm 0.03) + 0.90(\pm 0.02) M_w^A, \qquad (15)$$

where the superscripts S and A stand for Solfatara and Astroni, respectively. Therefore, the local and moment magnitudes can be evaluated for earthquakes recorded at the ASB2 station, using (9) and (10), respectively, and then this value can be corrected by using (14) or (15) to minimize possible bias introduced by different local site responses.

Discussion and Conclusion

In the present study we have calibrated the magnitude scales based on the earthquake coda duration for the Campi Flegrei area. These scales can be routinely applied because they allow rapid and fast magnitude estimates by simply picking the earthquake duration, so their use is suitable for real-time applications.

The advantage of calculating local (or moment) magnitudes from the coda duration, instead of making amplitude measurements, is that problems related to the saturation of the seismic traces that often occur with the most energetic earthquakes and that usually affect low-dynamic gain analog stations are fully overcome. This is particularly important for the routine magnitude estimates for the Campi Flegrei local earthquakes, because the reference station STH used at the INGV–OV is a low-dynamic analog instrument. Moreover, the local magnitude estimation through seismic amplitude by the use of (9) would also require trace manipulation to deconvolve the instrument response at first and then to convolve the signals with the Wood–Anderson seismometer transfer function. Finally, the earthquake location has to be known to estimate the distance-correction term.

On the other hand, it could happen that magnitude evaluations through (12) and/or (13) are not possible, for three main reasons:

1. A malfunction of the STH reference station;
2. In case of seismic swarms, when the very close temporal occurrence of the earthquakes prevents an estimation of the correct coda duration;
3. The amplitude of the seismic noise (or volcanic tremor) is high enough to mask the real coda duration of low-energy earthquakes.

To allow magnitude estimates in these cases also, the relationships between the magnitudes evaluated at the Solfatara and the Astroni sites, where the ASB2 digital station is located, have been obtained, providing an alternative to the STH reference analog station. By using equation (9), or alternatively (10), M_L and M_w can be evaluated for the Astroni site, and then by using the derived relations of equation (14) or (15), it can be traced back to the Solfatara site, to ensure the catalog homogeneity and consistency.

The advantage in using data from a digital station is that the application of equations (9) or (10) is always possible because the high-dynamic-range station is not affected by problems of saturation, and therefore local and moment magnitudes can be determined independently from the coda duration. This is important, because in environments with high seismic noise, like the highly urbanized and densely

populated Campi Flegrei area, the magnitude estimate based on the measurement of the ground-motion amplitude is more reliable than the duration-based magnitude estimate, especially for small events where the duration could be strongly biased when the noise level is high (see, for example, Del Pezzo *et al.*, 2003). The opportunity of calculating the magnitude through amplitude measurements is also particularly relevant in an active volcanic area like Campi Flegrei, where volcanic tremors related to episodes of possible unrest could mask the earthquake coda duration and therefore introduce bias in the duration-based magnitude estimates.

A final consideration concerns the moment magnitude scale. This scale represents the most objective way of estimating the earthquake energy, because it depends on the value of the seismic moment, and unlike the local scale, it does not depend on a normalization distance. Moreover, as seen in the previous sections, the absolute errors on M_{w} for earthquakes recorded with low signal-to-noise ratios are lower than those estimated for M_{L}. Therefore, the use of this scale is strongly recommended.

The local and moment magnitude scales discussed in this study were derived by correcting the amplitudes of the seismic signals for path and site effects, in order to obtain reliable quantification of the earthquake energy. As the local and moment magnitude estimates allow a comparison with earthquakes recorded in other volcanic areas, we believe that the scales presented should be applied routinely to the Campi Flegrei local seismicity. Moreover, due to its volcanological history, its geographic setting and its high degree of urbanization, the Campi Flegrei caldera is potentially one of the most high-risk volcanic areas in the world. Correct and reliable magnitude estimates are therefore necessary for quantitative evaluations of the volcano dynamics and are more urgent considering the recent episode of unrest that started in 2004.

Acknowledgments

We wish to thank F. Bianco, Gail Atkinson, David Boore, Christa von Hillebrande-Andrade, and an anonymous reviewer for the useful comments and suggestions that we believe have greatly improved this manuscript. The staff of the Monitoring Center of the INGV–OV is acknowledged for maintaining the database of the seismic waveforms. The present study is part of the activities of the Advanced Seismological Analysis Laboratory (LAV) of the INGV–OV.

References

Abercrombie, R. E. (1995). Earthquake source scaling relationships from −1 to 5 M_L using seismograms recorded at 2.5-km depth, *J. Geophys. Res.* **100,** 24,015–24,036.

Alsaker, A., L. B. Kvamme, R. A. Hansen, A. Dahle, and H. Bungum (1991). The M_L scale in Norway, *Bull. Seismol. Soc. Am.* **81,** 379–398.

Anderson, J. G., and S. E. Hough (1984). A model for the shape of the Fourier amplitude spectrum of acceleration at high frequencies, *Bull. Seismol. Soc. Am.* **74,** 1969–1993.

Aster, R. C., and R. P. Meyer (1988). Three-dimensional velocity structure and hypocenter distribution in the Campi Flegrei caldera, Italy, *Tectonophysics* **149,** 195–218.

Aster, R. C., R. P. Meyer, G. De Natale, A. Zollo, M. Martini, E. Del Pezzo, R. Scarpa, and G. Iannaccone (1992). Seismic investigation of Campi Flegrei caldera, in *Volcanic Seismology*, in Proceedings in Volcanology, Vol. **3**, Springer-Verlag, New York.

Bakun, W. H. (1984). Seismic moments, local magnitudes, and coda-duration magnitudes for earthquakes in central California, *Bull. Seismol. Soc. Am.* **74,** 439–458.

Baumbach, M., D. Bindi, H. Grosser, C. Milkereit, S. Parolai, R. Wang, S. Karakisa, S. Zünbül, and J. Zschau (2003). Calibration of an M_L scale in Northwestern Turkey from 1999 Izmit aftershocks, *Bull. Seismol. Soc. Am.* **93,** 2289–2295.

Bindi, D., D. Spallarossa, C. Eva, and M. Cattaneo (2005). Local and duration magnitudes in Northwestern Italy, and seismic moment versus magnitude relationships, *Bull. Seismol. Soc. Am.* **95,** 592–604.

Boatwright, J. (1978). Detailed spectral analysis of two small New-York state earthquakes, *Bull. Seismol. Soc. Am.* **68,** 1117–1131.

Boore, D. M. (1983). Stochastic simulation of high frequency ground motion based on seismological models of the radiated spectra, *Bull. Seismol. Soc. Am.* **73,** 1865–1894.

D'Amico, S., and V. Maiolino (2005). Local magnitude estimate at Mt. Etna, *Ann. Geophys.* **48,** 215–229.

Del Pezzo, E., and S. Petrosino (2001). A local-magnitude scale for Mt. Vesuvius from synthetic Wood-Anderson seismograms, *J. Seism.* **5,** 207–215.

Del Pezzo, E., F. Bianco, and G. Saccorotti (2003). Duration magnitude uncertainty due to seismic noise: inferences on the temporal pattern of G-R b-value at Mt. Vesuvius, Italy, *Bull. Seismol. Soc. Am.* **93,** 1847–1853.

Del Pezzo, E., S. De Martino, M. T. Parrinello, and C. Sabbarese (1993). Seismic site amplification factors in Campi Flegrei, Southern Italy, *Phys. Earth Planet. Inter.* **78,** 105–117.

De Natale, G., G. Iannaccone, M. Martini, and A. Zollo (1987). Seismic sources and attenuation properties at the Campi Flegrei volcanic area, *Pure Appl. Geophys.* **125,** 883–917.

Gasperini, P. (2002). Local magnitude revaluation for recent Italian earthquakes (1981–1996), *J. Seism.* **6,** 503–524.

Grünthal, G., and R. Wahlström (2003). An M_w based earthquake catalogue for central, northern and northwestern Europe using a hierarchy of magnitude conversions, *J. Seism.* **7,** 507–531.

Hanks, T. C., and D. M. Boore (1984). Moment-magnitude relations in theory and practice, *J. Geophys. Res.* **89,** 6229–6235.

Hanks, T. C., and H. Kanamori (1979). A moment-magnitude scale, *J. Geophys. Res.* **84,** 2348–2350.

Havskov, J., J. A. Pena, J. M. Ibanez, L. Ottemoller, and C. Martinez-Arevalo (2003). Magnitude scales for very local earthquakes. Application for Deception Island Volcano (Antarctica), *J. Volcanol. Geotherm. Res.* **128,** 115–133.

Hutton, L. K., and D. M. Boore (1987). The M_L scale in Southern California, *Bull. Seismol. Soc. Am.* **77,** 2074–2094.

Kim, W. Y. (1998). The M_L scale in eastern North America, *Bull. Seismol. Soc. Am.* **88,** 935–951.

Lay, T., and T. C. Wallace (1995). *Modern Global Seismology*, Academic Press, London.

Menke, W. (1984). *Geophysical Data Analysis: Discrete Inverse Theory*, Academic Press, New York.

Orsi, G., L. Civetta, C. Del Gaudio, S. de Vita, M. A. Di Vito, R. Isaia, S. M. Petrazzuoli, G. P. Ricciardi, and C. Ricco (1999). Short-term ground deformations and seismicity in the resurgent Campi Flegrei caldera (Italy): an example of active block-resurgence in a densely populated area, *J. Volcanol. Geotherm. Res.* **91,** 415–451.

Papazachos, B. C., A. A. Kiratzi, and B. G. Karacostas (1997). Toward a homogeneous moment-magnitude determination for earthquakes in Greece and the surrounding area, *Bull. Seismol. Soc. Am.* **87,** 474–483.

Richter, C. F. (1935). An instrumental earthquake magnitude scale, *Bull. Seismol. Soc. Am.* **25,** 1–32.

Saccorotti, G., S. Petrosino, F. Bianco, M. Castellano, D. Galluzzo, M. La Rocca, E. Del Pezzo, L. Zaccarelli, and P. Cusano (2007). Seismicity associated with the 2004–2006 renewed ground uplift at Campi Flegrei caldera, Italy, *Phys. Earth Planet. Inter.* **165,** 14–24.

Sato, H., and M. Fehler (1998). *Seismic Wave Propagation and Scattering in the Heterogeneous Earth*, Springer-Verlag, New York, 41–62.

Scordilis, E. M. (2006). Empirical global relations converting M_S and m_b to moment magnitude, *J. Seism.* **10,** 225–236.

Stange, S. (2006). M_L determination for local and regional events using a sparse network in Southwestern Germany, *J. Seism.* **10,** 247–257.

Vanorio, T., J. Virieux, P. Captano, and G. Russo (2005). Three-dimensional seismic tomography from P wave and S wave microearthquake travel times and rock physics characterization of the Campi Flegrei caldera, *J. Geophys. Res.* **110,** B03201, doi 10.1029/2004JB003102.

Istituto Nazionale di Geofisica e Vulcanologia
Sezione di Napoli Osservatorio Vesuviano
Via Diocleziano, 328
80124 Naples, Italy

Manuscript received 23 May 2007